Research Article

ZrO_2 Nanoparticles Filler-Based Mixed Matrix Polyethersulfone/Cellulose Acetate Microfiltration Membrane for Oily Wastewater Separation

Sura Mawlood Abbas and Sama Mohammed Al-Jubouri*
Department of Chemical Engineering, College of Engineering, University of Baghdad, Baghdad, Iraq

* Corresponding author. E-mail: sama.al-jubouri@coeng.uobaghdad.edu.iq, OrcID: 0000-0001-5080-411X
DOI: 10.14416/j.asep.2024.10.001
Received: 24 July 2024; Revised: 26 August 2024; Accepted: 16 September 2024; Published online: 1 October 2024

Abstract
Membrane technology has emerged as a dynamic field of study in academia and industry for treating produced oily wastewater. ZrO_2 nanoparticles (ZrO_2 NPs) filler-based mixed matrix polyethersulfone/cellulose acetate microfiltration membranes were fabricated and inspected in the oily wastewater remediation. The fabricated bare PES membrane, PES/CA blended polymers membrane, and PES/CA blended polymers incorporating ZrO_2 NPs (ZrO_2@PES/CA) membranes by phase inversion technique were inspected by field emission scanning electron microscopy, atomic force microscopy, Fourier-transform infrared spectroscopy, and measurement of water contact angle and porosity. The ZrO_2@PES/CA membrane which consisted of 0.5 wt.% ZrO_2 NPs (0.5%ZrPC) afforded increased hydrophilicity and reduced water contact angle from 70° for P membrane to 30.23°. Also, the 0.5%ZrPC membrane gave pure water flux of 88.89 L/m^2.h, high oil rejection of 98.2% and showed remarkable antifouling capacity with a high flux recovery ratio of 89.3% and relative flux reduction of 34.3%. The effect of transmembrane pressure (1, 2, 3, and 4 bar), feed temperature (25, 40, and 50 °C), and an initial oil concentration (250, 500, 750, and 1000 mg/L) on the permeation flux and oil rejection of the 0.5%ZrPC membrane was investigated. The results revealed that ZrO_2@PES/CA membranes have a significant potential for effective oil removal with high permeability and antifouling ability. The 0.5%ZrPC membrane confirmed its durability and reusability when kept an acceptable oil removal after 5 cycles.

Keywords: Cellulose acetate, Microfiltration, Oily wastewater, Polyethersulfone, Reusability, Zirconium oxide

1 Introduction

Wastewater is produced in substantial quantities from numerous industries, such as petrochemical, textile, metals, metallurgical, and food processing [1], [2]. The World Water Development Report 2017 published by the United Nations states that the agricultural, industrial and domestic sectors produce a considerable amount of wastewater and consume 70, 22 and 8% of the freshwater, respectively that is available worldwide [3]. According to the United Nations Educational, Scientific and Cultural Organization (UNESCO) report, over 80% of wastewater is not treated prior to it being discharged into the water body [4], [5]. Oily wastewater is characterized as wastewater containing significant concentrations of fats, oils, greases, and diverse ranges of dissolved organic and inorganic components in suspension [6]. Oil-contaminated wastewater represents a significant threat to both human health and the environment due to the hazardous properties it possesses. Therefore, treating this wastewater is an important issue [7], [8]. Various methods are employed to treat oily wastewater, such as filtration, flotation, adsorption, electrolysis, biochemistry, coagulation, gravity separation, skimming, and membrane separation [9]–[13]. Membrane technology is a highly promising method for treating wastewater, specifically oily wastewater [14]. Membrane technology has several benefits, including minimal energy usage, a small and efficient design, easy operation, the ability to be scaled up, and the potential

for continuous operation [15]. The utilization of a wide variety of membranes in diverse applications has demonstrated that the membrane technology is capable of successful retention of oil from water. The membrane separation technique, for instance, has been claimed to be applicable in the oil refining industry for the purpose of deacidification and degumming [16]. Earlier studies have reported the utilization of membrane technology for treating oily wastewater in vegetable oil factories [17], petroleum industries [18], and other industries that contain oil [19], [20].

Membrane separation methods are commonly categorized according to their pore sizes and the pressure at which they are operated. Pressure-driven membrane processes include microfiltration (MF), ultrafiltration (UF), nanofiltration (NF), and reverse osmosis (RO) [21], [22]. Polymeric and ceramic (inorganic) materials are typically used in the manufacturing of simple membranes. Polyethersulfone (PES), polysulfone (PSf), polyacrylonitrile (PAN), polyvinylidene fluoride (PVDF), polypropylene (PP), polyvinyl chloride (PVC) and cellulose acetate (CA) are frequently used polymers in the synthesis of polymeric membranes [23]. In general, they are cost-effective, exhibit an acceptable removal efficiency, and require low energy. The drawbacks of these membranes include the occurrence of fouling which raises the hydraulic resistance, decreases the flux and filtration capacity, decreases the membrane's lifetime, and consequently increases the operation costs [24]–[26]. The membrane's properties and overall performance are adversely affected by fouling, which is defined as the accumulation of dirt particles such as dissolved staff, or colloids on the membrane surface or inside its pores [27]. Therefore, it becomes necessary to develop the membrane structure to achieve the ultimate duty of the used membranes. Creating a hydrophilic surface helps in avoiding fouling either by coating a hydrophilic layer or alteration of the membrane structure by hydrophilic additives [28], [29]. To improve the membrane's texture, these membranes have been altered either by incorporation of additives or blending a polymer with another polymer. Many fabrication techniques, including phase-inversion, interfacial polymerization, stretching, track-etching, and electrospinning are usually used [30]. The phase inversion method type non-solvent induced phase inversion technique (NIPS) is the prevalent technique among other preparation methods of polymer membranes [31], [32]. The NIPS technique involves the immersion of the cast film in the coagulation solution that contains a non-solvent, resulting in an exchange of solvent and non-solvent [33], [34].

The PES is a suitable polymer type for the preparation of MF and UF membranes which are used in pressure-driven filtration processes identified as potential wastewater treatment methods [35], [36]. PES offers desirable quality membranes for oily wastewater treatment, but its hydrophobic features promote organic particle deposition on the membrane surface, clogging the pores, increasing the energy requirements and shortening the lifetime of the membrane [37]. PES possesses sulfone groups and ether bonds that alternate between aromatic rings. This molecular structure provides a significant degree of surface modification resulting in desirable properties such as creep resistance, high rigidity, strength, and a stable dimension structure [38]. The incorporation of hydrophilic polymers like poly(ethylene glycol) (PEG), poly(vinyl pyrrolidone) (PVP), polyethylenimine (PEI), polyvinyl alcohol (PVA), and CA [39] into the polymeric membranes serves as pore formers improving the performance of the membranes in terms of their water permeability and membrane wettability. Enhancing the hydrophilicity of the membranes is in favor of reducing their separation performance [40].

Cellulose acetate (CA) has been incorporated into various membrane types. CA is highly resistant to contamination because of its hydrophilicity [41]. Furthermore, CA is not favorable to aggressive cleaning due to its minimal chemical resistance and low mechanical strength [42]. To solve these problems, blending the polymer with inorganic additives has become a common method for developing new blended membranes with desirable features. There is an exponential increase in the incorporation of nanoparticles (NPs) into polymeric membrane matrix as a result of their distinctive characteristics, including their large surface area, high reactivity, and degree of functionalization for the treatment of wastewater [43]. The fabrication of mixed matrix membranes (MMMs) by integrating hydrophilic nanoparticles with hydrophobic polymer matrix has gained substantial attention because MMMs are easy to prepare, and have long-term operational stability and superior separation performance in terms of their permeability, rejection and antifouling properties [44], [45]. Therefore, the incorporation of inorganic nanoparticles (NPs) including alumina (Al_2O_3), titanium oxide (TiO_2), zirconium oxide (ZrO_2), silica (SiO_2), zinc oxide (ZnO), zeolite, and graphene oxide (GO) [46]–[50] into the polymeric membranes decreases the membranes

contact angle and enhances their hydrophilicity, hence improving the efficiency of pollutants separation. ZrO_2-containing membranes are considered more suitable for liquid phase applications in severe environments due to their chemical stability, which surpasses that of TiO_2 and Al_2O_3-containing membranes [51]. ZrO_2 NPs-containing PES/CA blended membranes for treating oily wastewater will be used for the first time in this study. ZrO_2 NPs-containing membranes were used for other specific issues such as the PES-PAA-ZrO_2 membrane used for polycyclic aromatic hydrocarbon removal [37], CA-ZrO_2 membrane used for protein removal [52], and PES/ZrO_2 for membrane bioreactor application [51].

A new generation of membranes can be obtained by embedding blended polymers with inorganic fillers. The resultant membrane from an organic/ inorganic combination would exhibit improved structure properties in terms of high hydrophilicity, mechanical strength, separation performance, and durability. In addition to the development of novel membrane materials and processes, the future directions of research should also consider the significance of the circular economy and sustainability concepts. Membrane technology can make an enormous impact on the reusability of water from various sources, gas separation for carbon capture, sustainable industrial development, and sustainable solutions in the health and energy fields [53]–[55].

The current study investigates the strategy of improving the PES MF membranes for oily wastewater separation by blending with CA and adding ZrO_2 NPs. In this context, the NIPS method was used to fabricate the polymer casting solution. The fabricated membranes were characterized by field emission scanning electron microscopy, atomic force microscopy, Fourier-transform infrared spectroscopy, porosity, and water contact angle tests. The efficacy of the prepared membranes was inspected at ranges of initial oil concentrations, solution temperature, and transmembrane pressure (TMP). Also, the reusability of the fabricated membrane was examined using an SDS cleaning solution.

2 Materials and Methods

2.1 *Materials*

PES $(C_{12}H_8O_3S)_n$, MW_n = 58,000 Da) was provided by O-BASF USA. CA is a hydrophilic polymer provided by CDH (P) Ltd. (MW_n = 30,000 Da. ZrO_2 NPs with a mean diameter of 35.9 nm (Figure S1) purchased from Shanghai Macklin Biochemical Co., Ltd. were used as the inorganic additive. Dimethylformamide (DMF) ($HCON(CH_3)_2$, 99.0% assay) is a solvent provided by Romil. Sodium dodecyl sulfate (SDS) ($CH_3(CH_2)_{11}OSO_3Na$, 99.0% assay) is a cleanser for the used membrane provided by Thomas Baker Chemical. Ltd. Synthetic oily wastewater was composed by homogenizing a kerosene and de-ionized water (DI) with a 9:1 (wt./wt.) ratio of kerosene to SDS [56]. SDS acted as a stabilizing surfactant for the oil in water under 1000 rpm of mixing for about 30 min until a homogeneous solution was obtained [57]. Kerosene, a model polluting oil, was provided by the Al-Daura refinery and its characteristics are depicted in Table S1. The Image-J software and the electronic microscope were used to analyze the oil droplet size distribution in the oil solution and the mean diameter was found to be 13.6 μm as shown in Figure S2.

2.2 *Membranes fabrication*

The bare PES membrane (P), PES/CA blended polymers membrane (PC), and ZrO_2@PES/CA membranes (ZrPC) were fabricated by the NIPS method. The casting solutions composition is presented in Table 1. A certain amount of ZrO_2 NPs was first dispersed in DMF solvent. Dried PES polymer was then added to the mixture and stirred at 400 rpm for 3 h until a homogenous solution was obtained. CA was then added to the solution with stirring for 12 h to generate a homogenous solution. The dope solution of the bare PES membrane was prepared in the same way but without adding ZrO_2 NPs and CA. Also, the PC membrane was fabricated in the same method but without ZrO_2 NPs. The viscosity of the dope solutions was estimated via a rapid Viscometer model Brookfield, CAP 2000, USA.

The flat sheet membranes were cast with a thickness of 200 μm via a film applicator device. An appropriate amount of the dope solution was cast over a smooth flat glass plate which was then immersed in a DI water bath to achieve the phase inversion at room temperature. After that, the fabricated membrane peeled off normally from the glass plate. Then, the membrane was moved to another water bath where it was left for about 24 h to completely remove the residual solvent.

Table 1: The composition of the casting solutions.

Membrane Code	PES (wt.%)	CA (wt.%)	ZrO_2 (wt.%)	DMF (wt.%)
P	17.00	-	-	83.00
PC	17.00	5.00	-	78.00
0.5%ZrPC	17.00	5.00	0.50	77.50
1%ZrPC	17.00	5.00	1.00	77.00
3%ZrPC	17.00	5.00	3.00	75.00

2.3 *MF system*

The MF experiments to evaluate the efficacy of the designed membranes were carried out in a crossflow system displayed in Figure 1 at 25 °C, TMP of 2 bar, and 0.9 L/min feed flow rate. The effective membrane area was 18 cm^2.

2.4 *Membrane characterization*

The field emission scanning electron microscopy (FESEM) provides important details about the morphology of the surface and cross-section of the composed membranes. This characterization was conducted using FESEM (ZEISS model device). A piece of the fabricated membrane was submerged in liquid nitrogen for a few minutes to freeze-fractured. The piece was then coated with gold before scanning. The Atomic Force Microscopy (AFM) technique using an Angstrom Advanced Inc., CSPM device was employed to map the topography of the membrane surface. The mapping was conducted to determine the average surface roughness (R_a), root mean square roughness (R_q) and pore size of the membrane. The Fourier-transform infrared spectroscopy (FT-IR) was performed to investigate the chemical structure of the membranes and their functionalities. This characterization was conducted using INVENIO, a microscope instrument with a spectrum range of 400–4000 cm^{-1}, and an optical resolution of 5–10000 pixels. The water contact angle (WCA) of membranes was measured to evaluate the membrane hydrophilicity. This characterization was performed by precisely dropping DI water on the membrane surface to be visualized by the model OCA 15 plus device. The gravimetric technique was employed to determine the membrane porosity ε% [12] according to Equation (1) [23].

$$\varepsilon\% = \frac{w_1 - w_2}{\rho \times A \times T} \times 100 \quad (1)$$

Where w_1 and w_2 are the weight of the wet and dry membrane (g), respectively. A is the membrane's area (cm^2), T is the membrane's thickness (cm) determined based on the obtained FESEM images, and ρ is the water density (g/cm^3).

2.5 *Performance evaluation*

The water permeation and separation performance of the fabricated MF membranes were determined using a crossflow testing rig. For evaluation and comparison of the permeability efficacy, the MF membranes were initially compacted utilizing DI water for 30 min at 3 bar. The TMP was then fixed at 2 bar and the pure water flux (PWF) of each membrane was measured according to Equation (2).

$$J = \frac{V}{A \times t} \quad (2)$$

Where V represents the permeate volume (L), t represents the time of filtration (min), and A represents the active membrane's area (m^2). Following the PWF measurement, the separation performance was conducted. A volume of the solutions with a 500 mg/L oil feed concentration was passed through the selected membrane at a TMP of 2 bar. The permeate flux, J_1 ($L/m^2.h$) was determined according to Equation 2. C_F and C_P are the concentrations of the oily wastewater in the feed and permeate. Both were measured by the Turbidimeter instrument (Lovibond TurbDirect, Germany).

The oil rejection (R%) was determined according to Equation (3).

$$R\% = \left(1 - \frac{C_P}{C_F}\right) \times 100 \quad (3)$$

The antifouling property of the fabricated membranes was evaluated by measuring the percentage of water flux recovery after fouling by oily wastewater. The flux recovery ratio (FRR%) and relative flux reduction (RFR%) were determined according to Equations (4) and (5), respectively.

$$FRR\% = \left(\frac{J_2}{J_o}\right) \times 100 \quad (4)$$

$$RFR\% = \left(1 - \frac{J_1}{J_o}\right) \times 100 \quad (5)$$

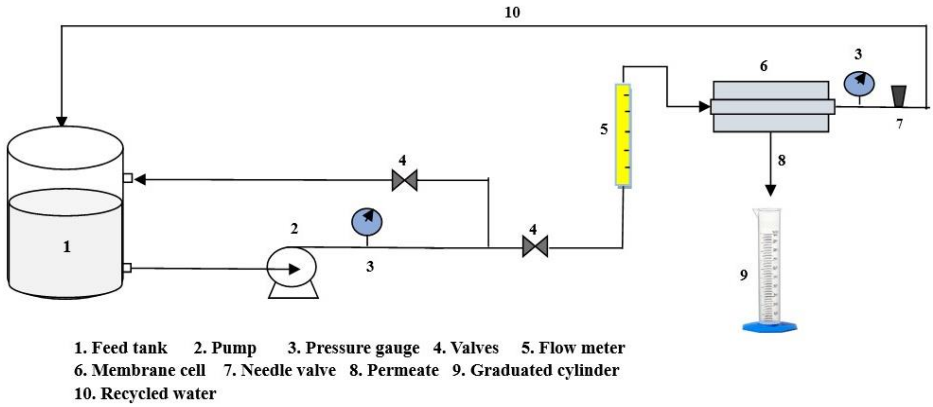

Figure 1: The experimental MF system.

Where J_o (L/m^2.h) is the PWF recorded for 1 h at a fixed TMP of 2 bar before fouling. Next, the water was replaced by 500 mg/L oily wastewater and the flux (J_1) was recorded for 1 h. Later, the used membrane was washed by steeping for 1 h in the SDS solution, followed by 30 min in DI water to remove the SDS residues. Ultimately, the PWF (J_2) of the washed membrane was measured for a further 1 h. The membrane, which gave the highest permeate flux and the best oil rejection was chosen to investigate the membrane's reusability in the removal of oily wastewater. The cleaning solution of 5 mM SDS was used to wash and regenerate the used membrane. The membrane was soaked in the SDS solution for 1 h followed by 30 min in DI water to be used later in the filtration process.

The membrane fouling is affected by the membrane's surface charge and the charge of the oily wastewater. If the oil droplet charge is similar to the surface charge of the membrane then the occurring repulsion will prevent the membrane from fouling, otherwise, the membrane fouling occurs [58]. Therefore, it becomes important to estimate the point of zero charge (pH_{zc}) at which the membrane surface has zero net charge and ΔpH of the electrolyte solution equals zero [59]. To determine the pH_{zc}, small pieces of 0.5%ZrPC membrane each with 2×2 cm^2 were suspended in 20 mL of 0.1 M NaCl solutions at different solution pH of 2–12. The solution pH was altered by 0.1 M HCl solution and 0.1 M NaOH solution. After shaking the containers for 48 h, the final pH of the solution was recorded. The values of ΔpH were plotted relative to the initial pH.

3 Results and Discussion

3.1 *Precast solution properties*

The viscosity is an essential parameter in membrane fabrication due to its influence on the solvent-non-solvent exchange rate and, consequently, the membrane's final morphology [60]. Table 2 shows the viscosity of the precast solutions of P, PC, and ZrPC membranes. Adding 5 wt.% of CA to the precast solution increased the viscosity from 255 cp to 877 cp. Incorporating both CA and ZrO_2 NPs in the polymeric solutions raised their viscosity substantially from 255 cp to 1867 cp. The highest viscosity was obtained for the 3%ZrPC membrane. A high concentration of additive increased the viscosity of the casting solution due to the corresponding rise in the polymer entanglement, which caused a delay in the exchange between the solvent and non-solvent during the NIPS process [61], [62]. Mei *et al*., [63] demonstrated that macrovoid formation was inhabited by solutions with a higher viscosity and vice versa. Padilha and Borges [64] synthesized membranes with 11, 14, 17, and 20 wt.% of PVC. They showed that the higher concentration of PVC of 20 wt.% increased the viscosity and altered the morphology of the membrane from a macroviod structure to a sponge-like structure. Alpatova *et al*., [60] demonstrated that the incorporation of nAg and PVP of 5 wt.% increased the viscosity of the casting solution. This resulted in the suppression of the formation of macrovoids in the membrane matrix due to a delay in the exchange rate. These findings agree with similar results obtained by Saki and Uzal [39].

Table 2: The viscosity of the precast solution.

Membrane Code	P	PC	0.5% ZrPC	1% ZrPC	3% ZrPC
Viscosity (cp)	255	877	1298	1830	1867

3.2 *Membrane characterization*

The top surface and cross-section morphology of the fabricated membranes are shown in Figure 2. The top surface of the P membrane shows a smooth surface with obvious openings, but the PC membrane shows the presence of white points on the top surface and the openings became relatively very fine, which indicates that the CA was successfully incorporated into the PES matrix. The effect of variation in the ZrO_2 NPs content in the casting solution at 0.5, 1, and 3 wt.% was observed on the top surface of the ZrPC membranes. Figure 2 shows the 0.5%ZrPC membrane has a relatively smooth surface with a few surface defects due to the simultaneous presence of ZrO_2 NPs and CA in the membrane texture. Furthermore, as the concentration of ZrO_2 NPs increased further to 1% and 3%, the distribution of nanoparticles on the top surface increased and became disfigured. This uneven distribution caused by agglomeration of the particles may affect the membrane's filtration performance.

The cross-section FESEM images in Figure 2 show that all the composed membranes have an asymmetric structure. The P and PC membranes consist of a dense layer on the top surface supported by a random finger-like structure and a sponge structure below the finger-like layer. The P and PC membranes exhibited almost similar cross-section structures with closed ends finger-like pores. However, the ZrO_2@PES/CA membranes showed numerous wider connected finger-like pores and many irregular macro-voids across the whole thickness. The variations in the cross-sectional structures can be attributed to adding ZrO_2 NPs and CA to the PES matrix altered the physical properties of the casting solution, such as the hydrophilicity and viscosity. The viscosity of the casting solution increased significantly as the dosage of ZrO_2 NPs increased, as shown in Table 1. This increase in viscosity restricts the solvent and nonsolvent diffusion and instantaneous de-mixing because it obstacles water diffusion to the lower layers of the casting solution. As a result, precipitation occurs at a slower rate, the structure of the membranes transformed into a finger-like structure with large macrovoids, and a large population of macro-voids formed because of the slow phase inversion kinetics. The same findings were illustrated in previous publications [65], [66]. The phase inversion kinetics was accelerated for both P and PC membranes because of the lower viscosity of the casting solution. Hence, the separation of the solvent and non-solvent phases took place early, and the formation of large voids was incomplete.

The AFM test and roughness parameters (R_a and R_q) of the membrane are displayed in Figure 3 and Table S2. These parameters were applied to assess the topography of the prepared membrane surfaces. The AFM images confirm that P and PC membranes have a smoother structure than the ZrO_2@PES/CA membranes. The R_a of the membrane increased with adding ZrO_2 NPs to the precast solution. The R_a values gradually rose from 23.7 nm for the P membrane to 57.57 nm for the 0.5%ZrPC membrane. Higher roughness typically affects the surface properties of the modified membrane in terms of increasing the filtration area of the membrane and decreasing the performance of the membrane against fouling [67]. Adding more than 0.5 wt.% of ZrO_2 NPs to the casting solution caused lower roughness because of the reduced surface porosity and pore size of the produced membrane as shown in Table S2. These results are similar to those reported by Abbas and Al-Jubouri [68] and Evangeline *et al*. [69].

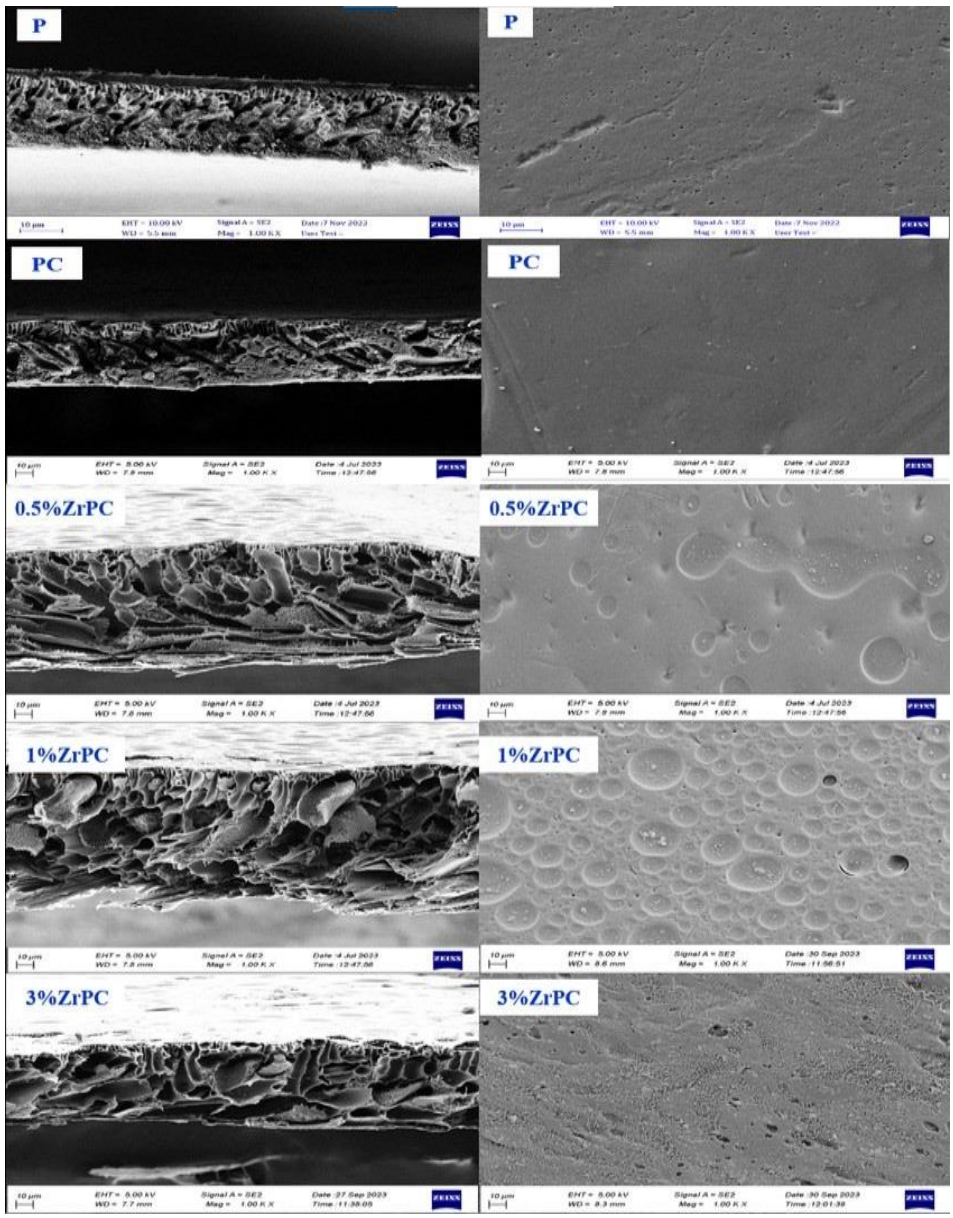

Figure 2: FESEM images of the cross-section and surface of the P, PC, and ZrPC membranes. (Scale bar is 10 µm).

The FT-IR spectroscopy is an effective device that can be used to investigate the structure, bonding, and reactivity of a matter. Figure 4 shows the FT-IR spectra of the fabricated membranes. The absorption peaks of =C-H, C-C, and C=C in the aromatic ring appeared at 3097.86, 1492 and 1577.7 cm^{-1} for P, PC, and ZrPC membranes. The symmetric stretching vibration of S=O, the asymmetric stretching vibration of S=O, and the C-O-C stretching vibration are represented by the peaks that appeared at 1149, 1319, and 1010 cm^{-1}, respectively. The FT-IR spectra for the PC membrane, the broad peaks at around 3500 cm^{-1} indicate O-H stretching vibrations due to the hydroxyl groups in CA. The C=O band was visible at around 1747 cm^{-1}, which could be attributed to the ester group of CA. When compared with the P membrane, the FT-IR bands of ZrPC membranes were shown to exhibit a consistent increase in the intensity of the absorption

peaks in the spectrum. The broad peaks observed around 3500–3600 are characteristic of hydroxyl group O-H stretching vibrations. This can be attributed to the enhanced hydrophilicity resulting from the presence of ZrO_2 NPs and CA. Peaks of the C=O band appeared around 1740–1750 cm^{-1}. Additionally, the newly detected peaks can be observed just below 1000 cm^{-1}, an absorption around 850 cm^{-1} which could be assigned to the vibration of the Zr-O functional group. The spectrum indicates a successful blending of PES, CA, and ZrO_2 NPs, as demonstrated by the O-H stretching vibration and the appearance of new peaks.

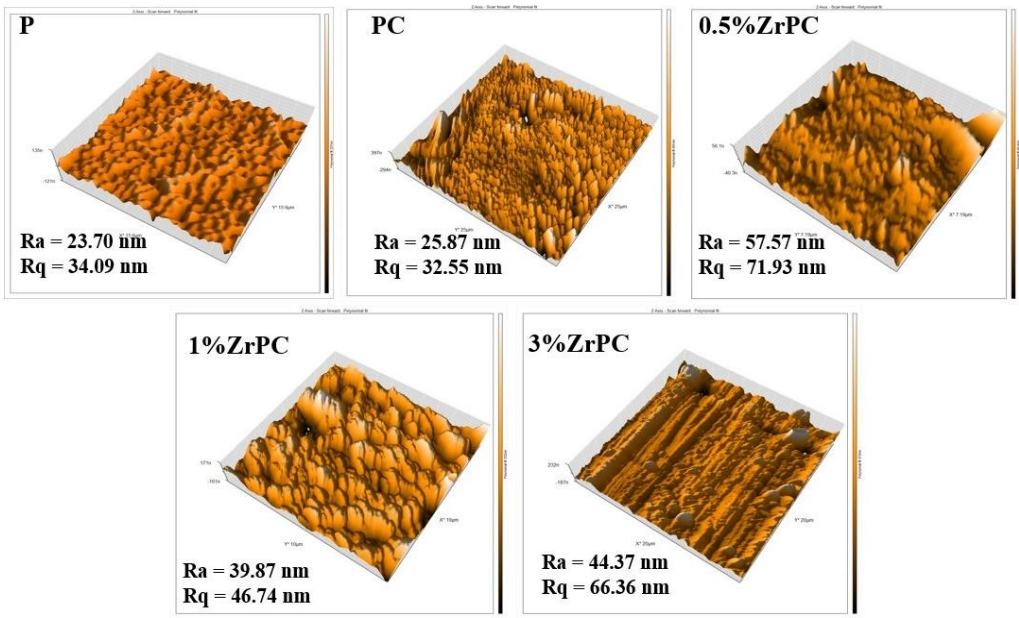

Figure 3: 3-dimension AFM images of the modified membranes.

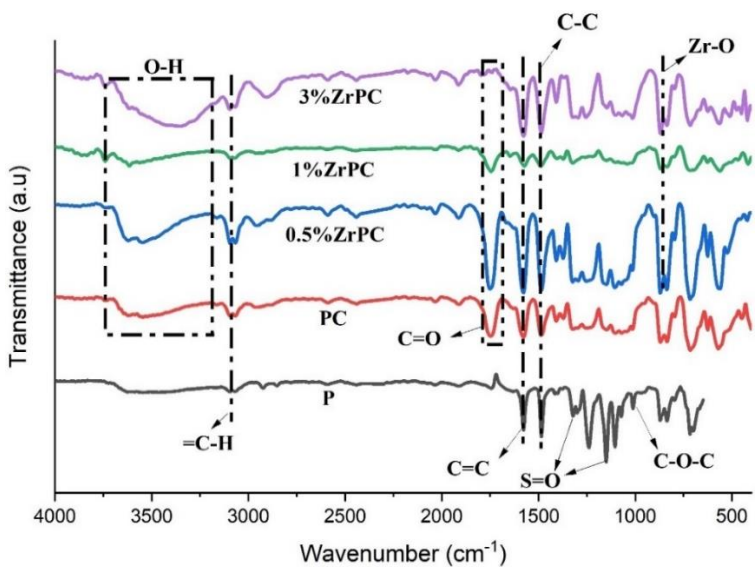

Figure 4: FT-IR spectra of the prepared membranes.

The thickness and porosity of P, PC, and ZrPC membranes are shown in Table 3. The results demonstrated that adding ZrO_2 NPs and CA to the casting solution increased the thickness of the membranes. The membrane thickness achieved maximum values of 169.766 μm for 3%ZrPC, which is thought to be caused by the high viscosity of the casting solution [70]. Adding ZrO_2 NPs to the PES/CA blend polymer caused a significant increase in the membrane thickness, which continued with raising the ZrO_2 NPs content to 3%. However, the absolute increase in the membrane thickness is not favorable because of increasing the resistance to molecular transfer across the membrane. According to Table 3 and Table S2, the porosity and pore size of ZrPC membranes were higher than that of the P and PC membranes. The porosity increased with the contribution of nanoparticles in the membrane. It is known that high porosity favors water flux. As a general rule increased exchange rates between water and solvent produce more porous membranes and vice versa [71]. The high porosity observed in the 0.5%ZrPC membrane can be attributed to the presence of an appropriate concentration of the hydrophilic additive in the membrane. This additive interacts with the polymer solution and facilitates the transport of solvent molecules from the polymer matrix to the coagulation bath [72]. At the same time, further increasing of ZrO2 NPs in the precast solution highly increased its viscosity as shown in Table 2. Viscous precast solution caused delayed de-mixing process, and slow precipitation rate during the coagulation process [73], [74], therefore reduced porosity was obtained for both 1%ZrPC and 3%ZrPC membranes. These results agreed with those obtained by Evangeline *et al*. [69].

Table 3: The thickness and porosity of the prepared membranes.

Membrane Code	P	PC	0.5% ZrPC	1% ZrPC	3% ZrPC
Thickness (μm)	83.75	127.205	135.86	154.51	169.766
ε%	44.5	60.2	88.8	78	76

The incorporation of CA and ZrO_2 NPs into the casting solution significantly impacts the membrane's morphology and the membrane's hydrophilicity. The WCA analysis was employed to quantify the hydrophilicity of the fabricated membrane. Figure 5(a) displays the WCA of the fabricated membrane. The P membrane exhibited the highest WCA of 70°. Adding CA into the casting solution led to a significant drop in the WCA to 44.6°. This is due to the hydroxyl and acetyl groups of the CA, which increase the hydrophilic nature of the fabricated membranes relative to other membranes. Furthermore, it was observed that ZrPC membranes have the lowest WCA due to the hydrophilic nature of ZrO_2 NPs, and CA added to the casting solution reduced the WCA to 30.23° for 0.5%ZrPC membrane. However, the WCA value increased to 37.4, and 42.95 for 1%ZrPC and 3%ZrPC membranes, respectively. This increase might be due to ZrO_2 agglomeration and uneven distribution of nanoparticles on the surface of the membrane. The WCA characteristic is essential for oily wastewater treatment because it determines the permeability and the ability of oil adhesion. Low WCA enhances the separation efficiency and prolongs the lifespan of the membrane [51].

3.3 *Performance of membranes*

Figure 5(b) presents the permeability performance of the P, PC, and ZrPC membranes during the MF process examined at a TMP of 2 bar, a temperature of 25 °C, and a flow rate of 0.9 L/min for 60 min. According to the results, the permeability was improved by adding CA and ZrO_2 NPs. The results show that the PWF using P membrane was 12.77 $L/m^2.h$, which can be assigned to the high WCA that it has and its low porosity. The PWF of the PC membrane was 47.2 $L/m^2.h$ because it contains 5 wt.% of CA polymer within the PES matrix which enhanced the hydrophilicity of the membrane. The PWF was improved by incorporating both ZrO_2 NPs and CA in the membrane matrix. The PWF value was 88.8, 38.3, and 49.4 $L/m^2.h$ using 0.5%ZrPC, 1%ZrPC, and 3%ZrPC membranes, respectively. The 0.5%ZrPC membrane afforded the highest PWF because of its low WCA and containing large connected macro-voids within its structure, which facilitated the water molecules' diffusion, and its high roughness, which increased the area of filtration. The PWF of the 1%ZrPC and 3%ZrPC decreased slightly which was expected based on their characteristics consisting of reduced porosity and moderated WCA in comparison with 0.5%ZrPC membrane.

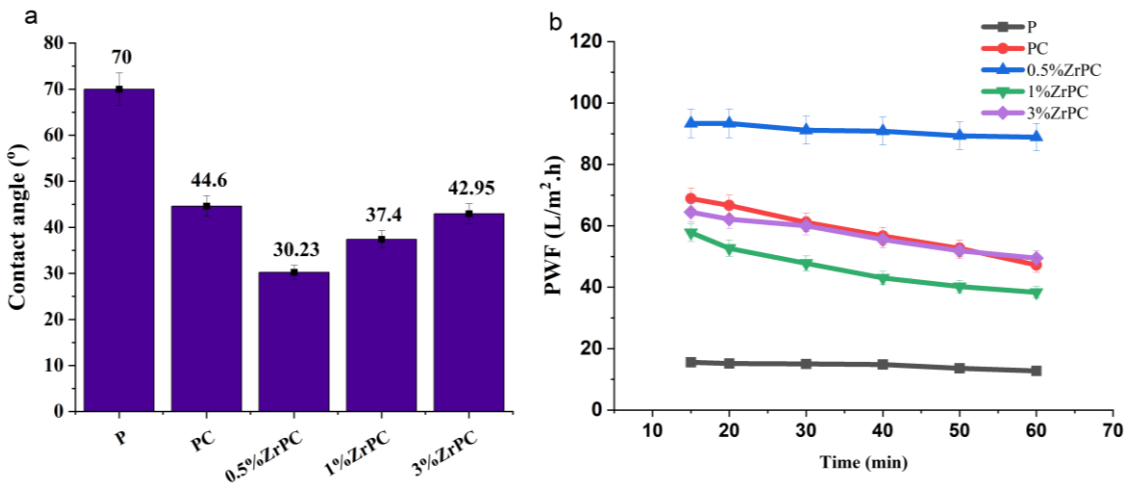

Figure 5: (a) Contact angle, (b) PWF of the prepared membrane.

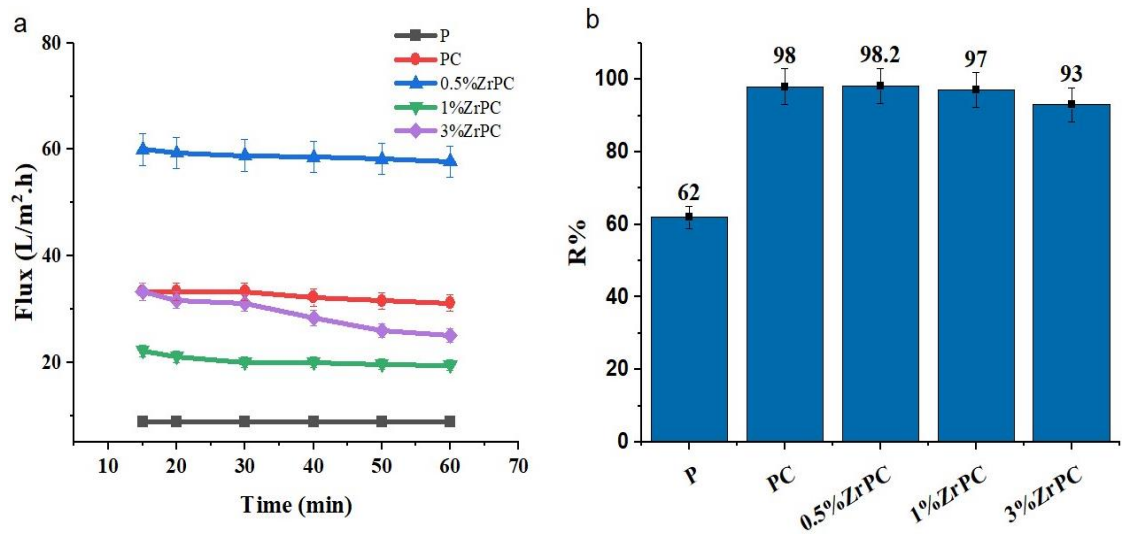

Figure 6: (a) Permeation flux, (b) oil rejection of the modified membrane.

Figure 6 shows the permeation flux and oil rejection of the fabricated membranes examined at an oil feed concentration of 500 mg/L, a temperature of 25 °C, a TMP of 2 bar, and a flow rate of 0.9 L/min for 60 min. The permeation flux increased by adding CA and ZrO_2 NPs up to 0.5 wt.% and then slightly decreased with adding more ZrO_2 NPs. Figure 6a shows that the permeation flux of the fabricated membrane increased from 8.88 L/m^2.h for the P membrane to 57.77 L/m^2.h for the 0.5%ZrPC membrane. The modified membrane with ZrO_2 NPs exhibited better permeation flux compared to the P membrane as a result of the enhanced hydrophilicity that these additives achieved. The oil rejection given by all modified membranes was higher than that given by the P membrane. The PC, 1%ZrPC, and 3%ZrPC membranes showed high oil rejection of 98%, 97%, and 93%, respectively, but low permeation flux due to their low porosity and aggregation of nanoparticles on the top surface. The high efficiency of the 0.5%ZrPC membrane can perhaps be due to the uniform distribution of ZrO_2 NPs, which increased the hydrophilicity of the membrane as confirmed by the low WCA and enhanced the membrane's permeability.

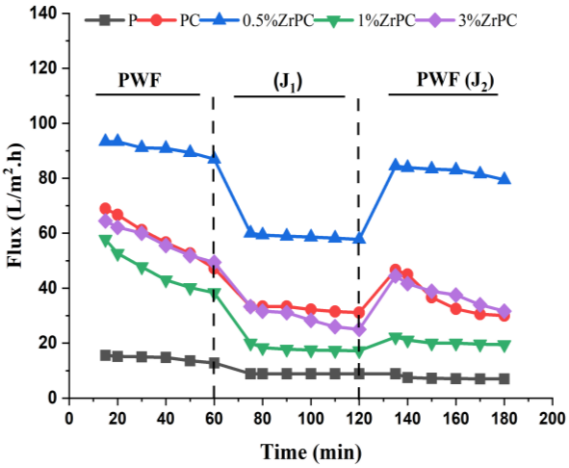

Figure 7: Time−dependent water permeation fluxes during the fouling processes.

Fouling is one of the most frequent issues associated with membrane applications in wastewater treatment. The rapid build-up of oil droplets due to adsorption and deposition on the membrane surface results in direct membrane fouling. The PWF before and after the MF process were investigated to determine the usability of the fabricated membrane [39], [75]. The flux of the prepared membranes measured pre- and post-filtration of oily wastewater is shown in Figure 7. When the pure water was replaced with an oily wastewater solution, the flux of the membranes declined with time as shown in Figure 7 due to the adsorption of oil on the surface of the membrane, which led to obstruction of the membrane pores. However, the PWF was restored when the membrane was washed with SDS solution. The results show that the 0.5%ZrPC membrane has a good performance in comparison with other fabricated membranes. This can be attributed to its high hydrophilicity which boosts the membrane antifouling property. Also, Figure 7 shows that the PWF of the cleaned P membrane was not restored and continuously declined below the permeate of oily wastewater. This result confirms the necessity of blending PES with hydrophilic additives for oily wastewater treatment to overcome its hydrophobicity. The same trend was observed for the cleaned 1%ZrPC despite its initial high PWF referring to avoiding using ≥ 1 wt% of ZrO_2 NPs in the PES/CA matrix.

Figure 8(a) shows the FRR% and RFR% of the composed membranes. The FRR% of the P, PC, 0.5%ZrPC, 1%ZrPC, and 3%ZrPC membranes was 54.3%, 58.2%, 89.3%, 44.9%, and 64%, respectively. Also, the RFR% of the P, PC, 0.5%ZrPC, 1%ZrPC, and 3%ZrPC membranes was 30.4%, 34.1%, 34.3%, 49.2%, and 49.4%, respectively. The high FRR% and low RFR% of the 0.5%ZrPC membrane indicate that the membrane's antifouling characteristics have been significantly improved. Antifouling performance is typically considered favorable when RFR% is low and FRR% is high. The variation in filtration efficiency among these membranes can be attributed to the surface characteristics of the membranes and the variation of their hydrophilicity [76].

The reusability was investigated in cyclic procedures because it is a crucial parameter of membrane performance. SDS was utilized as a cleanser because SDS is semi-soluble in both organic and aqueous solvents and contains both hydrophobic and hydrophilic groups. By surrounding macromolecules in micelles, surfactants can solubilize them and eliminate foulants from the membrane surface [59]. Figure 8(b) presents the results of the membrane reusability obtained at an oil feed concentration of 500 mg/L, a TMP of 2 bar, and a feed solution temperature of 25 °C. It was observed that there was a slight reduction in oil removal efficiency (82%) after up to five cycles using the 0.5%ZrPC membrane. The oil removal efficiency dropped sharply to 60.5% after seven cycles of regeneration. This indicates that after successive usage, the membrane permitted the passage of oil particles through its pores during the separation of oily wastewater because the pores became larger. Also, the reduction in the percentage of oil removed can be attributed to occurring irreversible fouling, which cannot be eliminated during washing and oil accumulation which can lead to occurring concentration polarization. These results agreed with those obtained by Tahazadeh *et al*. [77].

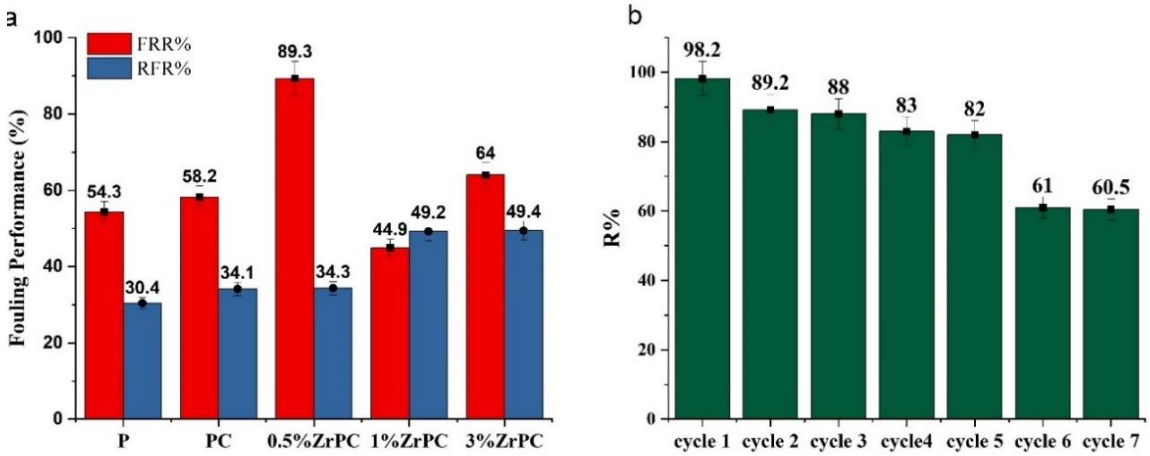

Figure 8: (a) FRR% and RFR% for the prepared membranes, (b) Reusability of 0.5%ZrPC membrane.

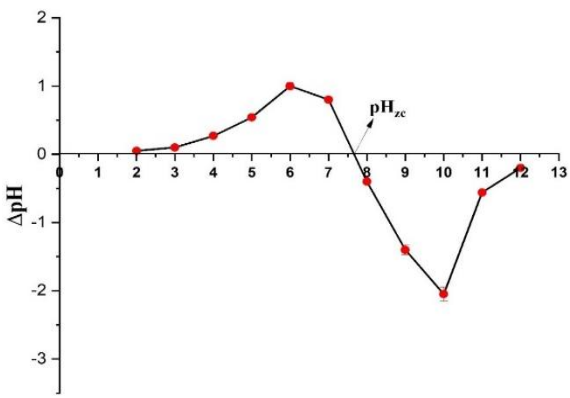

Figure 9: The pH_{zc} of the 0.5%ZrPC membrane.

The point of zero charge (pH_{zc}) should explain the behavior of 0.5%ZrPC membrane in the oily wastewater separation. The plot of ΔpH versus initial pH is shown in Figure 9. The pH_{zc} of the 0.5%ZrPC membrane was determined at pH = 7.6. The surface charge of this membrane is positive at pH below the pH_{zc} and passes through the pH_{zc} at which it has no charge. And it becomes negative at pH above the pH_{zc}. The pH of the kerosene feed solution is 7.18, and the surface charge of the membrane is highly positive at this value, so this condition is suitable for the separation process. This high positive charge caused the repulsion between the membrane surface and the oily wastewater solution made from kerosene which has a positively charged combination (alkanes C9–C16). Other studies reported that a neutral medium is more favorable to achieving a high removal percentage of kerosene having a pH of 7 [78], [79].

3.4 *Effect of TMP*

Figure 10 shows the TMP effect on the permeate flux and oil rejection using 0.5%ZrPC membrane at a temperature of 25 °C and a feed oil concentration of 500 mg/L. The influence of TMP on the performance of the membrane was investigated in the MF system at a TMP range of 1–4 bar. The permeate flux increased because of rising TMP, while the oil rejection was negatively affected by this increase. An increase in the applied pressure caused a corresponding rise in the permeate flux from 16.11 $L/m^2.h$ at 1 bar to 69.44 $L/m^2.h$ at 4 bar as seen in Figure 10a. Furthermore, the oil rejection after 1 h was 99%, 98.2%, 98%, and 91% at 1 bar, 2 bars, 3 bars, and 4 bars as shown in Figure 10(b). High TMP forced the oil droplets to move through the pores of the membrane at a faster rate and increased the amount of oil passing through the membrane. Therefore, less oil rejection was obtained. These results are in agreement with Masoudnia *et al*. [80].

3.5 *Effect of temperature of the feed solution*

The effect of temperature of the feed solution was investigated using 0.5%ZrPC membrane at temperatures of 25, 40, and 50 °C, TMP of 2 bar, and an oil feed concentration of 500 mg/L. The results presented in Figure 11 show that the flux rose as the temperature of the feed solution increased, whereas the oil rejection slightly decreased as the temperature increased. The increase in the temperature of the feed solution resulted in a substantial reduction in its viscosity, which consequently facilitates the oil passage through the membrane. This result agreed with the work done by Al-Alawy and Al-Musawi [81] and Makki *et al.* [82].

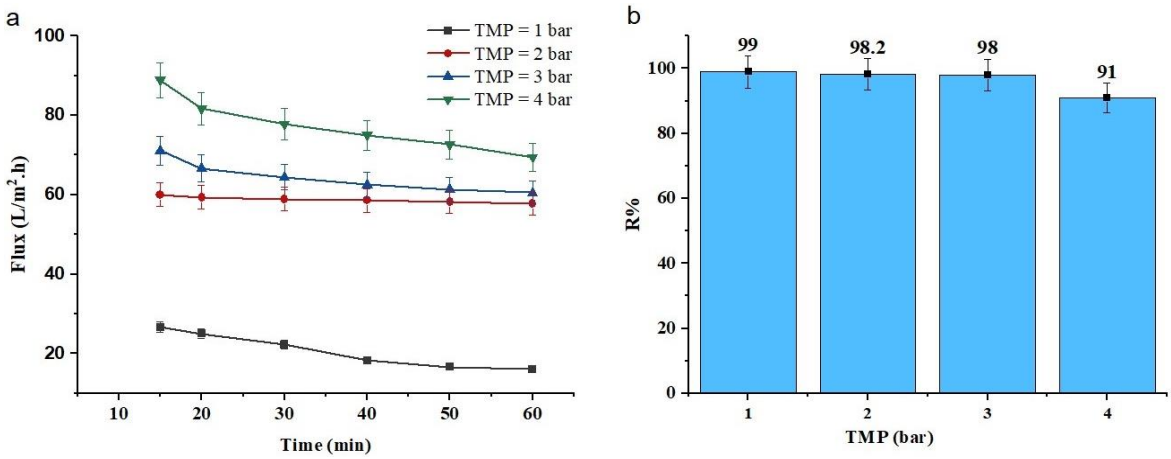

Figure 10: The effect of TMP on the (a) permeation flux, (b) oil rejection% using the 0.5%ZrPC membrane at an oil feed concentration of 500 mg/L and feed temperature of 25 °C.

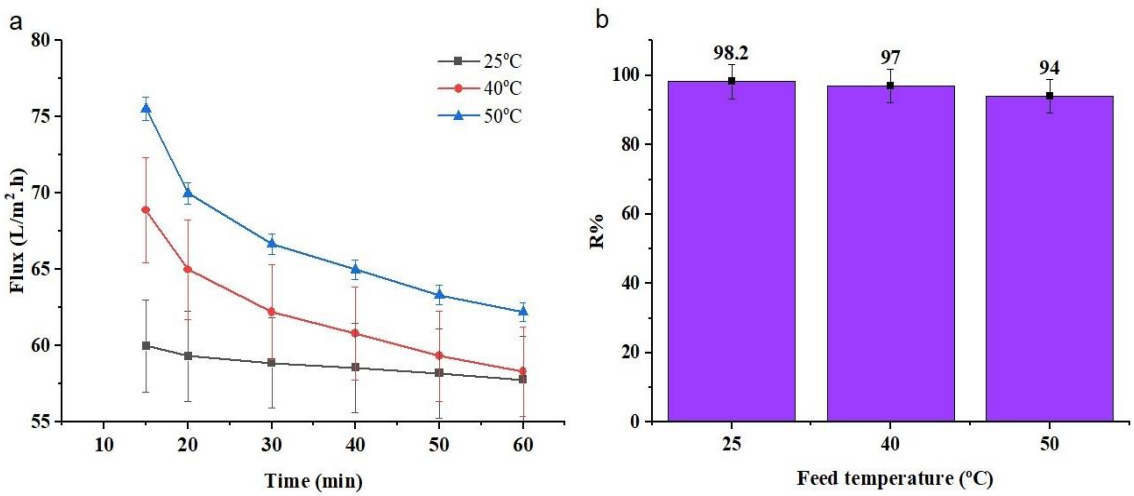

Figure 11: The effect of temperature of the feed solution on the (a) permeation flux, (b) oil rejection% using the 0.5%ZrPC membrane at an oil feed concentration of 500 mg/L and TMP of 2 bar.

3.6 *Effect of oil concentration*

Figure 12 shows the effect of oil concentration on the oil rejection and the permeate flux with time. This effect was studied at different oil concentrations of 250, 500, 750, and 1000 mg/L using the 0.5%ZrPC membrane at a feed temperature of 25 °C and TMP of 2 bar. The permeate flux exhibited a reduction as the oil feed concentration increased. The flux dropped from 63.33 L/m^2.h at 250 mg/L to 16.11 L/m^2.h at 1000 mg/L. These results demonstrate that the concentration of oil in the feed solution has a significant impact on increasing the hydraulic resistance and the degree of interaction between oil droplets and the membrane surface [83]. The rate of permeation through the membrane decreased because the accumulated oil layer on the membrane surface worked as an extra barrier drug the permeate and oil passage. Therefore, the oil rejection increased to over 97% as the oil content of the feed solution was changed from 250 to 1000 mg/L. This result well agreed with those obtained by Damayanti *et al*. [84].

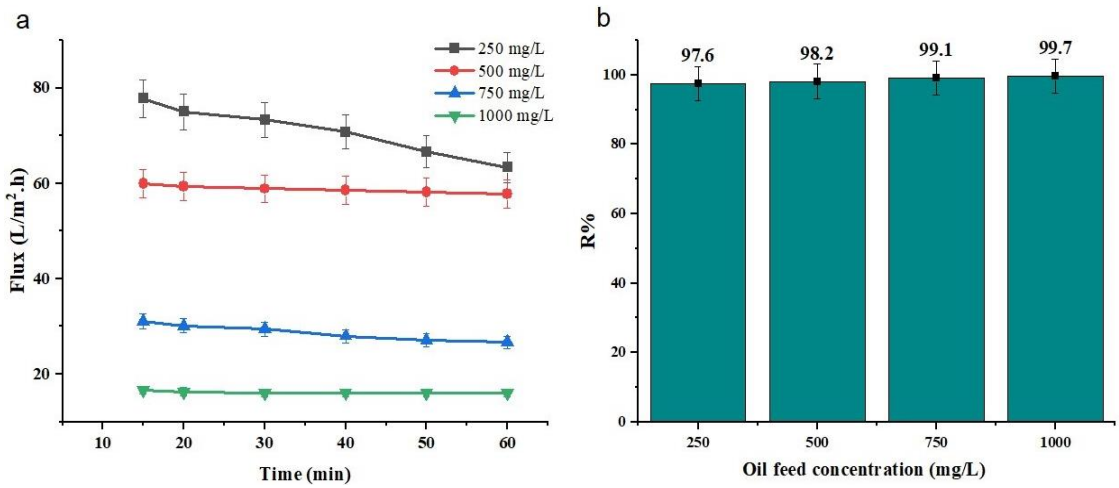

Figure 12: The effect of oil concentration on the (a) permeation flux, (b) oil rejection% using the 0.5%ZrPC membrane at feed temperature of 25 °C and TMP of 2 bar.

4 Comparison Study

The membrane separation performance of the PES membrane modified with CA and ZrO_2 NPs was compared to other membranes that utilized oily wastewater to evaluate the membrane's efficacy. This comparison is presented in Table 4. Based on the Permeation flux, oil rejection, and FRR%, the comparison is established. Therefore, the environmental and economic feasibility of oily wastewater treatment can be considerably improved by utilizing ZrO_2@PES/CA asymmetric membranes.

The development of high-performing and durable ZrO_2-based MMM can enhance the efficiency and sustainability of the separation processes and encourage the reuse of water. This could contribute to the reduction of environmental impact and carbon emissions, while also helping in the achievement of the United Nation's Sustainable Development Goals. Moreover, the ZrO_2@PES/CA membrane can be produced in more economical conditions if green agricultural sources are used to produce CA and ZrO_2 NPs for oil separation from wastewater.

On the other hand, several obstacles or constraints may arise when scaling up membrane technology for industrial applications such as material limitations based on durability and fouling effects, economic sustainability, which consists of cost of production and energy consumption, performance scaling of efficiency losses, and environmental and regularity restrictions like waste disposal and compliance with regulations.

5 Conclusions

In this study, (17 wt.%) PES and (5 wt.%) CA were blended with (0.5 wt.%, 1 wt.%, and 3 wt.%) ZrO_2 NPs to obtain mixed matrix MF membranes for the treatment of oily wastewater. The findings demonstrated that the incorporation of ZrO_2 NPs into the dope solution enhanced various characteristics of the obtained membranes, including resistance to contamination caused by oil deposition and adsorption, PWF, and oil rejection. The WCA decreased from 70° for the P membrane to 30.23° for the 0.5%ZrPC membrane. The efficacy of membranes was evaluated by PWF, oil rejection, permeation flux, FRR%, and RFR%, and they were 88.8 L/m^2.h, 98.2%, 57.7 L/m^2.h, 89.3%, and 34.3%, respectively, for the 0.5%ZrPC membrane. The permeate flux increased as the TMP and the temperature of the feed solution increased, while it decreased as the oil content in the feed solution increased. The oil rejection showed the inverse behavior of the permeate flux with increasing TMP, the temperature of the feed solution, and oil feed concentration. Investigation into the reusability of the 0.5%ZrPC membrane showed that the membrane could separate 82% of oil after 5 cycles using SDS as a cleanser.

Table 4: Comparison study in oily wastewater treatment.

Base Polymer	Additive	Oil Source	Concentration (mg/L)	Flux ($L/m^2.h$)	Rejection (%)	FRR (%)	Ref.
PES (17 and 12 wt.%)	PEG and CA/PEG	Kerosene	500	10 27	98 88	-	[85]
PSF (20 wt.%)	PEI/$CaCO_3$	Vacuum pump oil	1000	98	> 90%	100	[39]
PES (14 wt.%)	PVP/n-SiO_2	oil	2000	149.7	98	-	[35]
PVC (15 wt.%)	B-SiO_2	Crude oil	100	197.02	99.19	80.63	[23]
PVDF (15 wt.%)	PVP/PC	Commercial oil	88	28.59	97.80	-	[86]
PVC (15 wt.%)	SnO_2	Crude oil	100	104.06	99.3	91.57	[87]
PES (17 wt.%)	CA-ZrO_2	Kerosene	500	57.7	98.2%	89.3	This study

Author Contributions

S.M.A.: investigation, methodology, data curation, writing an original draft, research design, data analysis; S.M.A.: investigation, methodology, reviewing and editing, research design, data analysis, project administration. Both authors have read and agreed to the published version of the manuscript.

Conflicts of Interest

The authors declare no conflict of interest.

References

[1] T. Ahmad, X. Liu, and C. Guria, "Preparation of polyvinyl chloride (PVC) membrane blended with acrylamide grafted bentonite for oily water treatment," *Chemosphere*, vol. 310, 2023, Art. no. 136840, doi: 10.1016/j.chemosphere.2022.136840.

[2] S. Koushkbaghi, S. Jamshidifard, A. ZabihiSahebi, A. Abouchenari, M. Darabi, and M. Irani, "Synthesis of ethyl cellulose/aluminosilicate zeolite nanofibrous membranes for oil–water separation and oil absorption," *Cellulose*, vol. 26, no. 18, pp. 9787–9801, Dec. 2019, doi: 10.1007/s10570-019-02738-w.

[3] S. Putatunda, S. Bhattacharya, D. Sen, and C. Bhattacharjee, "A review on the application of different treatment processes for emulsified oily wastewater," *International Journal of Environmental Science and Technology*, vol. 16, no. 5, pp. 2525–2536, 2019, doi: 10.1007/s13762-018-2055-6.

[4] S. Hakak, W. Z. Khan, G. A. Gilkar, N. Haider, M. Imran, and M. S. Alkatheiri, "Industrial wastewater management using blockchain technology: Architecture, requirements, and future directions," *IEEE Internet of Things Magazine*, vol. 3, no. 2, pp. 38–43, 2020, doi: 10.1109/iotm.0001.1900092.

[5] K. Abuhasel, M. Kchaou, M. Alquraish, Y. Munusamy, and Y. T. Jeng, "Oilywastewater treatment: Overview of conventional and modern methods, challenges, and future opportunities," *Water (Switzerland)*, vol. 13, no. 7, 2021, doi: 10.3390/w13070980.

[6] A. I. Adetunji and A. O. Olaniran, "Treatment of industrial oily wastewater by advanced technologies: A review," *Applied Water Science*, vol. 11, no. 6, pp. 1–19, 2021, doi: 10.1007/s13201-021-01430-4.

[7] S. A. Sadek, S. M. Al-Jubouri, and S. Al-Batty, "Investigating the fouling models of the microfiltration mixed matrix membranes-based oxide nanoparticles applied for oil-in-water emulsion separation," *Iraqi Journal of Chemical and Petroleum Engineering*, vol. 25, no. 2, pp. 1–16, 2024, doi: 10.31699/ijcpe.2024.2.1.

[8] S. Jamaly, A. Giwa, and S. W. Hasan, "Recent improvements in oily wastewater treatment: Progress, challenges, and future opportunities," *Journal of Environmental Sciences*, vol. 37, pp. 15–30, 2015, doi: 10.1016/j.jes.2015.04.011.

[9] J. Lei and Z. Guo, "PES asymmetric membrane for oil-in-water emulsion separation," *Colloids and Surfaces A: Physicochemical and Engineering Aspects*, vol. 626, 2021, Art. no. 127096, doi: 10.1016/j.colsurfa.2021.127096.

[10] C. Sun, T. O. Leiknes, J. Weitzenböck, and B. Thorstensen, "Development of a biofilm-MBR for shipboard wastewater treatment: The effect of process configuration," *Desalination*, vol. 250, no. 2, pp. 745–750, 2010, doi: 10.1016/j.desal.2008.11.034.

[11] H. H. Sokker, N. M. El-Sawy, M. A. Hassan, and B. E. El-Anadouli, "Adsorption of crude oil from aqueous solution by hydrogel of chitosan based polyacrylamide prepared by radiation induced graft polymerization," *Journal of Hazardous Materials*, vol. 190, no. 1–3, pp. 359–365, 2011, doi: 10.1016/j.jhazmat.2011.03.055.

[12] H. N. Alfalahy and S. M. Al-Jubouri, "Preparation and application of polyethersulfone ultrafiltration membranincorporating NaX zeolite for lead ions removal from aqueous solutions," *Desalination and Water Treatment*, vol. 248, pp. 149–162, 2022, doi: 10.5004/dwt.2022.28072.

[13] M. H. Salih and A. F. Al-Alawy, "Crystallization process as a final part of zero liquid discharge system for treatment of east baghdad oilfield produced water," *Iraqi Journal of Chemical and Petroleum Engineering*, vol. 23, no. 1, pp. 15–22, 2022, doi: 10.31699/IJCPE.2022.1.3 1.

[14] A. E. Jery, A. Ahsan, S. S. Sammen, A. Shanableh, D. Sain, A. A. Ramírez-Coronel, M. A. Uddin, M. A. J. Maktoof, M. Shafiquzzaman, and N. Al-Ansari, "Industrial oily wastewater treatment by microfiltration using silver nanoparticle-incorporated poly (acrylonitrile-styrene) membrane," *Environmental Sciences Europe*, vol. 35, no. 1, 2023, doi: 10.1186/s12302-023-00764-x.

[15] N. Abdul, H. Nordin, A. F. Ismail, and N. Misdan, "Modified zeolite/polysulfone mixed matrix membrane for enhanced CO_2/CH_4 separation," *Membrane*, vol. 11, p. 630, 2021, doi: 10.3390/membranes11080630.

[16] C. de Morais Coutinho, M. C. Chiu, R. C. Basso, A. P. B. Ribeiro, L. A. G. Gonçalves, and L. A. Viotto, "State of art of the application of membrane technology to vegetable oils: A review," *Food Research International*, vol. 42, no. 5–6, pp. 536–550, 2009, doi: 10.1016/j.foodres.2009.02.010.

[17] T. Mohammadi and A. Esmaeelifar, "Wastewater treatment using ultrafiltration at a vegetable oil factory," *Desalination*, vol. 166, no. 1–3, pp. 329–337, 2004, doi: 10.1016/j.desal.2004.06.087.

[18] A. Salahi, I. Noshadi, R. Badrnezhad, B. Kanjilal, and T. Mohammadi, "Nano-porous membrane process for oily wastewater treatment: Optimization using response surface methodology," *Journal of Environmental Chemical Engineering*, vol. 1, no. 3, pp. 218–225, 2013, doi: 10.1016/j.jece.2013.04.021.

[19] A. Salahi, A. Gheshlaghi, T. Mohammadi, and S. S. Madaeni, "Experimental performance evaluation of polymeric membranes for treatment of an industrial oily wastewater," *Desalination*, vol. 262, no. 1–3, pp. 235–242, 2010, doi: 10.1016/j.desal.2010.06.021.

[20] B. Bolto, J. Zhang, X. Wu, and Z. Xie, "A review on current development of membranes for oil removal from wastewaters," *Membranes (Basel)*, vol. 10, no. 4, pp. 1–18, 2020, doi: 10.3390/membranes10040065.

[21] N. A. Ahmad, P. S. Goh, Z. A. Karim, and A. F. Ismail, "Thin film composite membrane for oily waste water treatment: Recent advances and challenges," *Membranes (Basel)*, vol. 8, no. 4, Oct. 2018, doi: 10.3390/membranes8040086.

[22] S. Yadav and S. Kamsonlian, "Progress on the development of techniques to remove contaminants from wastewater: A review," *Applied Science and Engineering Progress*, vol. 16, no. 3, 2023, Art. no. 6729, doi: 10.14416/j.asep.2023.02.001.

[23] S. A. Sadek and S. M. Al-Jubouri, "Structure and performance of polyvinylchloride microfiltration membranes improved by green silicon oxide nanoparticles for oil-in-water emulsion separation," *Materials Today Sustainability*, vol. 24, 2023, Art. no. 100600, doi: 10.1016/j.mtsust.2023.100600.

[24] A. Alammar, S. H. Park, C. J. Williams, B. Derby, and G. Szekely, "Oil-in-water separation with graphene-based nanocomposite membranes for produced water treatment," *Journal of Membrane Science*, vol. 603, 2020, Art. no. 118007, doi: 10.1016/j.memsci.2020.118007.

[25] S. Ghimire, M. Flury, E. J. Scheenstra, and C. A. Miles, "Sampling and degradation of biodegradable plastic and paper mulches in field after tillage incorporation," *Science of the Total Environment*, vol. 703, 2020, Art. no. 135577, doi: 10.1016/j.scitotenv.2019.135577.

[26] M. Zoubeik, M. Ismail, A. Salama, and A. Henni, "New Developments in Membrane Technologies Used in the Treatment of Produced Water: A Review," *Arabian Journal for Science and Engineering*, vol. 43, no. 5, pp. 2093–2118, 2018, doi: 10.1007/s13369-017-2690-0.

[27] A. I. Osman, Z. Chen, A. M. Elgarahy, M. Farghali, I. M. A. Mohamed, A. K. Priya, H. B. Hawash, and P. S. Yap, "Membrane technology for energy saving: Principles, techniques, applications, challenges, and prospects," *Advanced Energy and Sustainability Research*, vol. 5, no. 5, 2024, doi: 10.1002/aesr.202400011.

[28] S. M. Al-Jubouri, S. Al-Batty, R. K. S. Al-Hamd, R. Sims, M. W. Hakami, and M. H. SK, "Sustainable environment through using porous materials: A review on wastewater treatment," *Asia-Pacific Journal of Chemical Engineering*, vol. 18, no. 4, 2023, doi: 10.1002/apj.2941.

[29] M. H. Xu, R. Xie, X. J. Ju, W. Wang, Z. Liu, and L. Y. Chu, "Antifouling membranes with bi-continuous porous structures and high fluxes prepared by vapor-induced phase separation," *Journal of Membrane Science*, vol. 611, 2020, Art. no. 118256, doi: 10.1016/j.memsci.2020.118256.

[30] B. S. Lalia, V. Kochkodan, R. Hashaikeh, and N. Hilal, "A review on membrane fabrication: Structure, properties and performance relationship," *Desalination*, vol. 326, pp. 77–95, 2013, doi: 10.1016/j.desal.2013.06.016.

[31] X. Dong, D. Lu, T. A. L. Harris, and I. C. Escobar, "Polymers and solvents used in membrane fabrication: A review focusing on sustainable membrane development," *Membranes (Basel)*, vol. 11, no. 5, 2021, doi: 10.3390/membranes11050309.

[32] N. H. M. Safari, S. Rozali, A. R. Hassan, and R. Osman, "Inducing the skinned-oriented asymmetrical nanofiltration membranes via controlled evaporation times in dry/wet phase inversion process," *Applied Science and Engineering Progress*, vol. 16, no. 2, 2023, Art. no. 6015, doi: 10.14416/j.asep.2022.05.007.

[33] M. Khorsand-Ghayeni, J. Barzin, M. Zandi, and M. Kowsari, "Fabrication of asymmetric and symmetric membranes based on PES/PEG/DMAc," *Polymer Bulletin*, vol. 74, no. 6, pp. 2081–2097, 2017, doi: 10.1007/s00289-016-1823-z.

[34] A. G. Saleem and S. M. Al-Jubouri, "Efficient separation of organic dyes using polyvinylidene fluoride/polyethylene glycol-tin oxide (PVDF/PEG-SnO_2) nanoparticles ultrafiltration membrane," *Applied Science and Engineering Progress*, vol. 17, no. 4, 2024, Art. no. 7523, doi: 10.14416/j.asep.2024.08.001.

[35] M. B. Ghandashtani, F. Z. Ashtiani, M. Karimi, and A. Fouladitajar, "A novel approach to fabricate high performance nano-SiO_2 embedded PES membranes for microfiltration of oil-in-water emulsion," *Applied Surface Science*, vol. 349, pp. 393–402, 2015, doi: 10.1016/j.apsusc.2015.05.037.

[36] H. N. Alfalahy and S. M. Al-Jubouri, "A Comparison Study for The Performance of polyethersulfone ultrafiltration mixed matrix membranes in the removal of heavy metal ions from aqueous solutions," *Iraqi Journal of Chemical and Petroleum Engineering*, vol. 23, no. 2, pp. 19–25, 2022, doi: 10.31699/ijcpe.2022.2.3.

[37] X. Chen, G. Huang, C. An, R. Feng, Y. Wu, and C. Huang, "Superwetting polyethersulfone membrane functionalized with ZrO_2 nanoparticles for polycyclic aromatic hydrocarbon removal," *Journal of Materials Science and Technology*, vol. 98, pp. 14–25, 2022, doi: 10.1016/j.jmst.2021.01.063.

[38] M. Batool, A. Shafeeq, B. Haider, and N. M. Ahmad, "TiO_2 nanoparticle filler-based mixed-matrix PES/CA nanofiltration membranes for enhanced desalination," *Membranes (Basel)*, vol. 11, no. 6, 2021, doi: 10.3390/membranes11060433.

[39] S. Saki and N. Uzal, "Preparation and characterization of PSF/PEI/$CaCO_3$ nanocomposite membranes for oil/water separation," *Environmental Science and Pollution Research*, vol. 25, no. 25, pp. 25315–25326, 2018, doi: 10.1007/s11356-018-2615-9.

[40] I. C. Escobar and B. Van Der Bruggen, "Microfiltration and ultrafiltration membrane science and technology," *Journal of Applied Polymer Science*, vol. 132, no. 21, 2015, doi: 10.1002/app.42002.

[41] R. Abu-Zurayk, N. Alnairat, A. Khalaf, A. A. Ibrahim, and G. Halaweh, "Cellulose Acetate membranes: Fouling types and antifouling strategies—a brief review," *Processes*, vol. 11, p. 489, 2023, doi: 10.3390/pr11020489.

[42] K. J. Diainabo, N. H. Mthombeni, and M. Motsa, "Preparation and characterization of hybrids of cellulose acetate membranes blended with polysulfone and embedded with silica for Copper(II), Iron(II) and Zinc(II) removal from contaminated solutions," *Journal of Polymers and the Environment*, vol. 29, no. 11, pp. 3587–3604, 2021, doi: 10.1007/s10924-021-02094-6.

[43] B. Vani, M. Shivakumar, S. Kalyani, and S. Sridhar, "TiO_2 nanoparticles incorporated high-performance polyphenyl sulfone mixed matrix membranes for ultrafiltration of domestic greywater," *Iranian Polymer Journal*, vol. 30, no. 9, pp. 917–934, 2021, doi: 10.1007/s13726-021-00945-6.

[44] S. Mokhtari, A. Rahimpour, A. A. Shamsabadi, S. Habibzadeh, and M. Soroush, "Enhancing performance and surface antifouling properties of polysulfone ultrafiltration membranes with salicylate-alumoxane nanoparticles", *Applied Surface Science*, vol. 393, pp. 93–102, 2017, doi: 10.1016/j.apsusc.2016.10.005.

[45] E. Y. Kim, H. S. Kim, D. Kim, J. Kim, and P. S. Lee, "Preparation of mixed matrix membranes containing ZIF-8 and UiO-66 for multicomponent light gas separation," *Crystals*, vol. 9, no. 1, 2019, doi: 10.3390/cryst9010015.

[46] M. Abdullah and S. Al-Jubouri, "Implementation of hierarchically porous zeolite-polymer membrane for Chromium ions removal," in *IOP Conference Series: Earth and Environmental Science*, 2021. doi: 10.1088/1755-1315/779/1/012099.

[47] A. M. Asiri, V. Pugliese, F. Petrosino, S. B. Khan, K. A. Alamry, S. Y. Alfifi, H. M. Marwani, M. M. Alotaibi, D. Mukherjee, and S. Chakraborty, "Photocatalytic degradation of textile dye on blended cellulose acetate membranes," *Polymers (Basel)*, vol. 14, no. 3, 2022, doi: 10.3390/polym14030636.

[48] C. N. Matindi, M. Hu, S. Kadanyo, Q. V. Ly, N. N. Gumbi, D. S. Dlamini, J. Li, Y. Hu, Z. Cui, and J. Li, "Tailoring the morphology of polyethersulfone/sulfonated polysulfone ultrafiltration membranes for highly efficient separation of oil-in-water emulsions using TiO_2 nanoparticles," *Journal of Membrane Science*, vol. 620, 2021, Art. no. 118868, doi: 10.1016/j.memsci.2020.118868.

[49] S. M. Abdullah, "Oily water treatment using ceramic memberane," *Journal of Engineering*, vol. 17, no. 2, pp. 252–264, 2011.

[50] N. H. Ibrahim and S. M. Al-Jubouri, "Preparation and characterization of a hierarchically porous zeolite-carbon composite from economical materials and green method," *Iraqi Journal of Chemical and Petroleum Engineering*, vol. 24, no. 3, pp. 27–32, 2023, doi: 10.31699/IJCPE.2023.3.3.

[51] N. Maximous, G. Nakhla, W. Wan, and K. Wong, "Performance of a novel ZrO2/PES membrane for wastewater filtration," *Journal of Membrane Science*, vol. 352, pp. 222–230, 2010, doi: 10.1016/j.memsci.2010.02.021.

[52] G. Arthanareeswaran and P. Thanikaivelan, "Fabrication of cellulose acetate-zirconia hybrid membranes for ultrafiltration applications: Performance, structure and fouling analysis," *Separation and Purification Technology*, vol. 74, no. 2, pp. 230–235, 2010, doi: 10.1016/j.seppur. 2010.06.010.

[53] E. O. Ezugbe and S. Rathilal, "Membrane technologies in wastewater treatment: A review," *Membranes*, vol. 10, no. 5, p. 89, 2020.

[54] M. Issaoui, S. Jellali, A. A. Zorpas, and P. Dutournie, "Membrane technology for sustainable water resources management: Challenges and future projections," *Sustainable Chemistry and Pharmacy*, vol. 25, 2022, Art. no. 100590, doi: 10.1016/j.scp.2021.100590.

[55] A. Ali, E. Drioli, and F. Macedonio, "Membrane engineering for sustainable development: A perspective," *Applied Sciences*, vol. 7, no. 10, 2017, doi: 10.3390/app7101026.

[56] I. S. Al-Husaini, A. R. M. Yusoff, W. J. Lau, A. F. Ismail, M. Z. Al-Abri, B. N. Al-Ghafri, and M. D. H. Wirzal, "Fabrication of polyethersulfone electrospun nanofibrous membranes incorporated with hydrous manganese dioxide for enhanced ultrafiltration of oily solution," *Separation and Purification Technology*, vol. 212, pp. 205–214, 2019, doi: 10.1016/j.seppur.2018.10.059.

[57] R. J. Gohari, E. Halakoo, W. J. Lau, M. A. Kassim, T. Matsuura, and A. F. Ismail, "Novel polyethersulfone (PES)/hydrous manganese dioxide (HMO) mixed matrix membranes with improved anti-fouling properties for oily wastewater treatment process," *RSC Advances*, vol. 4, no. 34, pp. 17587–17596, 2014, doi: 10.1039/c4ra00032c.

[58] S. Huang, R. H. A. Ras, and X. Tian, "Antifouling membranes for oily wastewater treatment: Interplay between wetting and membrane fouling," *Current Opinion in Colloid and Interface Science*, vol. 36, pp. 90–109, 2018, doi: 10.1016/j.cocis. 2018.02.002.

[59] A. Salahi, T. Mohammadi, R. M. Behbahani, and M. Hemmati, "Asymmetric polyethersulfone ultrafiltration membranes for oily wastewater treatment: Synthesis, characterization, ANFIS modeling, and performance," *Journal of Environmental Chemical Engineering*, vol. 3, no. 1, pp. 170–178, 2015, doi: 10.1016/j.jece. 2014.10.021.

[60] A. Alpatova, E. S. Kim, X. Sun, G. Hwang, Y. Liu, and M. Gamal El-Din, "Fabrication of porous polymeric nanocomposite membranes with enhanced anti-fouling properties: Effect of casting composition," *Journal of Membrane Science*, vol. 444, pp. 449–460, 2013, doi: 10.1016/j.memsci.2013.05.034.

[61] W. M. Nielen, J. D. Willott, J. A. R. Galicia, and W. M. De Vos, "Effect of solution viscosity on the precipitation of PSaMA in aqueous phase separation-based membrane formation," *Polymers (Basel)*, vol. 13, no. 11, 2021, doi: 10.3390/ polym13111775.

[62] T. Rajasekhar, M. Trinadh, P. Veera Babu, A. V. S. Sainath, and A. V. R. Reddy, "Oil-water emulsion separation using ultrafiltration membranes based on novel blends of poly(vinylidene fluoride) and amphiphilic tri-block copolymer containing carboxylic acid functional group," *Journal of Membrane Science*, vol. 481, pp. 82–93, 2015, doi: 10.1016/j.memsci.2015.01.030.

[63] S. Mei, C. Xiao, and X. Hu, "Preparation of Porous PVC Membrane via a Phase Inversion Method from PVC/DMAc/Water/Additives," *Journal of Applied Polymer Science*, vol. 116, no. 5, pp. 2658–2667, 2011, doi: 10.1002/app.

[64] L. F. Padilha and C. P. Borges, "PVC membranes prepared via non-solvent induced phase separation process," *Brazilian Journal of Chemical Engineering*, vol. 36, no. 1, pp. 497–509, 2019, doi: 10.1590/0104-6632.20190361s20170132.

[65] Y. M. Zheng, S. W. Zou, K. G. N. Nanayakkara, T. Matsuura, and J. P. Chen, "Adsorptive removal of arsenic from aqueous solution by a PVDF/zirconia blend flat sheet membrane," *Journal of Membrane Science*, vol. 374, no. 1–2, pp. 1–11, 2011, doi: 10.1016/j.memsci.2011.02.034.

[66] H. Rabiee, S. Mojtaba Seyedi, H. Rabiei, N. Alvandifar, and A. Arya, "Preparation and characterization of PVC/PAN blend ultrafiltration membranes: Effect of PAN concentration and PEG with different molecular weight," *Desalination and Water Treatment*, vol. 58, pp. 1–11, 2017, doi: 10.5004/dwt.2017.0094.

[67] F. Kouhestani, M. A. Torangi, A. Motavalizadehkakhky, R. Karazhyan, and R. Zhiani, "Enhancement strategy of polyethersulfone (PES) membrane by introducing pluronic F127/graphene oxide and phytic acid/graphene oxide blended additives: Preparation, characterization and wastewater filtration assessment," *Desalination and Water Treatment*, vol. 171, pp. 44–56, 2019, doi: 10.5004/dwt.2019.24769.

[68] S. M. Abbas and S. M. Al-Jubouri, "High performance and antifouling zeolite@ polyethersulfone/cellulose acetate asymmetric membrane for efficient separation of oily wastewater," *Journal of Environmental Chemical Engineering*, vol. 12, no. 3, 2024, Art. no. 112775, doi: 10.1016/j.jece.2024.112775.

[69] C. Evangeline, V. Pragasam, K. Rambabu, S. Velu, P. Monash, G. Arthanareeswaran, and F. Banat, "Iron oxide modified polyethersulfone/ cellulose acetate blend membrane for enhanced defluoridation application," *Desalination and Water Treatment*, vol. 156, pp. 177–188, 2019, doi: 10.5004/dwt.2018.23174.

[70] D. Ghazanfari, D. Bastani, and S. A. Mousavi, "Preparation and characterization of poly (vinyl chloride) (PVC) based membrane for wastewater treatment," *Journal of Water Process Engineering*, vol. 16, pp. 98–107, 2017, doi: 10.1016/j.jwpe.2016.12.001.

[71] Z. Alhalili, C. Romdhani, H. Chemingui, and M. Smiri, "Removal of dithioterethiol (DTT) from water by membranes of cellulose acetate (AC) and AC doped ZnO and TiO_2 nanoparticles," *Journal of Saudi Chemical Society*, vol. 25, no. 8, 2021, doi: 10.1016/j.jscs.2021.101282.

[72] W. Fang, G. Liang, J. Li, and S. Guo, "Microporous formation mechanism of biaxial stretching PA6/PP membranes with high porosity and uniform pore size distribution," *Polymers (Basel)*, vol. 14, no. 11, 2022, doi: 10.3390/polym14112291.

[73] A. A. R. Abdel-Aty, Y. S. A. Aziz, M. G. A. Rehab, I. M. A. ElSherbiny, S. Panglisch, M. Ulbricht, and Ahmed S. G. Khalil, "High performance isotropic polyethersulfone membranes for heavy oil-in-water emulsion separation," *Separation and Purification Technology*, vol. 253, 2020, Art. no. 117467, doi: 10.1016/j.seppur.2020.117467.

[74] T. D. Kusworo, Qudratun, and D. P. Utomo, "Performance evaluation of double stage process using nano hybrid PES/SiO_2-PES membrane and PES/ZnO-PES membranes for oily waste water treatment to clean water," *Journal of Environmental Chemical Engineering*, vol. 5, pp. 6077–6086, 2017, doi: 10.1016/j.jece.2017.11.044.

[75] M. Ebrahimi, D. Willershausen, K. S. Ashaghi, L. Engel, L. Placido, P. Mund, P. Bolduan, and P. Czermak, "Investigations on the use of different ceramic membranes for efficient oil-field produced water treatment," *Desalination*, vol. 250, no. 3, pp. 991–996, 2010, doi: 10.1016/j.desal.2009.09.088.

[76] N. Gao and Z. K. Xu, "Ceramic membranes with mussel-inspired and nanostructured coatings for water-in-oil emulsions separation," *Separation and Purification Technology*, vol. 212, 2018, pp. 737–746, 2019, doi: 10.1016/j.seppur.2018.11.084.

[77] S. Tahazadeh, T. Mohammadi, and M. Ahmadzadeh, "Development of cellulose acetate /metal-organic framework derived porous carbon

adsorptive membrane for dye removal applications," *Journal of Membrane Science*, vol. 638, 2021, Art. no. 119692, doi: 10.1016/j.memsci.2021.119692.
[78] I. H. Dakhil, "Removal of kerosene from wastewater using locally sawdust," in *1st International Conference of Southern Technical University*, 2016, pp. 155–161.
[79] B. R. Simonović, D. Arandelović, M. Jovanović, B. Kovačević, L. Pezo, and A. Jovanović, "Removal of mineral oil and wastewater pollutants using hard coal," *Chemical Industry and Chemical Engineering Quarterly*, vol. 15, no. 2, pp. 57–62, 2009, doi: 10.2298/CICEQ0902057S.
[80] K. Masoudnia, A. Raisi, A. Aroujalian, and M. Fathizadeh, "A hybrid microfiltration/ultrafiltration membrane process for treatment of oily wastewater," *Desalination and Water Treatment*, vol. 55, no. 4, pp. 901–912, 2015, doi: 10.1080/19443994.2014.922501.
[81] A. F. Al-Alawy and S. M. A.–Musawi, "Microfiltration membranes for separating oil/water emulsion," *Iraqi Journal of Chemical and Petroleum Engineering*, vol. 14, no. 4, pp. 53–70, 2013, doi: 10.31699/IJCPE.2013.4.7.
[82] H. F. Makki, A. F. Al-Alawy, M. H. Al-Hassani, and Z. W. Rashad, "Membranes separation process for oily wastewater treatment," *Journal of Engineering*, vol. 17, no. 2, pp. 235–252, 2011.
[83] N. U. Barambu, M. R. Bilad, N. Huda, N. A. H. M. Nordin, M. A. Bustam, A. Doyan, and J. Roslan, "Effect of membrane materials and operational parameters on performance and energy consumption of oil/water emulsion filtration," *Membranes (Basel)*, vol. 11, no. 5, 2021, doi: 10.3390/membranes11050370.
[84] A. Damayanti, R. Z. Sholihah, T. K. Sari, N. Karnaningroem, and A. Moesriati, "The performance of restaurant wastewater treatment by using zeolite nanofiltration membrane," *ARPN Journal of Engineering and Applied Sciences*, vol. 14, no. 15, pp. 2670–2674, 2019.
[85] A. Mansourizadeh and A. Javadi Azad, "Preparation of blend polyethersulfone/cellulose acetate/polyethylene glycol asymmetric membranes for oil-water separation," *Journal of Polymer Research*, vol. 21, p. 375, 2014, doi: 10.1007/s10965-014-0375-x.
[86] M. A. Masuelli, "Ultrafiltration of oil/water emulsions using PVDF/PC blend membranes," *Desalination and Water Treatment*, vol. 53, no. 3, pp. 569–578, 2015, doi: 10.1080/19443994.2013.846539.
[87] S. A. Sadek and S. M. Al-Jubouri, "Highly efficient oil-in-water emulsion separation based on innovative stannic oxide/polyvinylchloride (SnO_2/PVC) microfiltration membranes," *Journal of Industrial and Engineering Chemistry*, In press, Jun. 2024, doi: 10.1016/j.jiec.2024.06.016.

Supporting Information

Table S1: Properties of processed kerosene from the Al-Daura refinery.

No.	Test	Value
1	Density at 15 °C g/cm^3	0.783
2	API	48.4
4	H_2S content mg/L	Nil
5	Mercapt. Sulphur wt.%	0.0254
6	Sulphur wt.%	0.21

Table S2: AFM results.

Membrane Type	Mean Pore Size (µm)	Average Surface Roughness (Ra) (nm)	Root Mean Square Height (Rq) (nm)
P	0.1125	23.70	34.09
PC	0.1533	25.87	32.55
0.5%ZrPC	0.1539	57.57	71.93
1%ZrPC	0.1431	39.87	46.74
3%ZrPC	0.1002	44.37	66.36

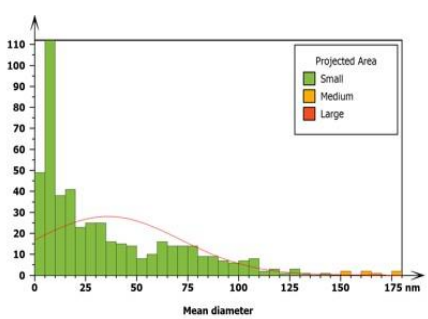

Figure S1: Particles size distributions for ZrO_2 NPs.

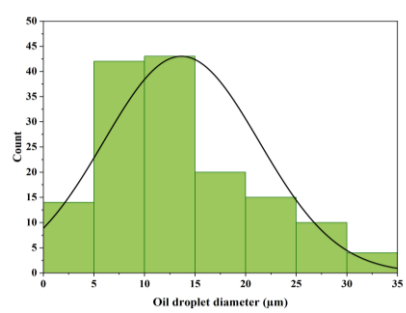

Figure S2: Oil droplet size distribution in the oily wastewater.